Theory of Structural Phase Transitions in a Trapped Coulomb Crystal

Daniel H. E. Dubin

Department of Physics, University of California at San Diego, La Jolla, California 92093-0319

(Received 6 April 1993)

Crystalline confined systems of charges exhibit structural phase transitions as a function of the anisotropy of the confining potential. A theory which describes these structural transitions is presented. The theory is based on the transitions which occur in infinite homogeneous 1D and 2D systems. These transitions have been previously explored for 1D systems but not for 2D systems. The charge density in the inhomogeneous crystal is found using a fluid theory as well as a theory which keeps correlations in the local density approximation.

PACS numbers: 64.70.−p, 61.50.−f

In several recent experiments [1–4] the technique of laser cooling applied to trapped ions has led to the formation of crystalline ionic systems of a single sign of charge. In this novel form of condensed matter, the ions are held together against their mutual Coulomb repulsion not by a neutralizing background of electrons, but rather by the external fields of a (radio-frequency) Paul [2–4] or (magnetic) Penning [1] trap. This unneutralized collection of ions represents the least dense (on the order of 10^8 cm^{-3}) form of condensed matter yet studied.

In most experiments the number of trapped ions is small ($N \lesssim 10^4$) so the crystalline system is inhomogeneous, and the structure of the crystal is affected by this inhomogeneity. For example, a Paul trap in a ring configuration has been used to trap a toroidal cloud of ions [4]. The ions are attracted to the circular ring axis by an external potential of the form $m\omega_r^2 r^2/2$, where r is distance from the axis, m is the ion mass, and ω_r is the radial oscillation frequency. For sufficiently large ω_r the ions form a 1D chain of equally spaced charges around the ring circumference. As ω_r decreases, Coulomb repulsion induces an instability in the chain wherein ions alternate in a zigzag pattern from one side of the ring axis to the other. As the radial force weakens further the zigzag develops a twist, forming a double helix that winds around the axis. A comparison of the energies of these structures predicts that the transitions occur when

$$(q^2/ma^3)^{1/2}/\omega_r = x_i\,, \tag{1}$$

where a is the axial spacing between charges of charge $q, x_1 = [7/\zeta(3)/2]^{1/2} = 2.05\ldots$ for the zigzag transition [5] and $x_2 = 1.29\ldots$ for the helical transition [6]. At lower transition values x_i more complex structures occur consisting of concentric cylindrical shells of ions [4–7].

The theory of the structural transitions in the ring map is simplified by the homogeneity of the torus in the azimuthal direction; that is, the charge per unit axial length does not vary. However, in many traps the ions are confined in a harmonic external potential of the form $\phi(r,z) = m(\omega_r^2 r^2 + \omega_z^2 z^2)/2$, where z measures distance along the trap axis, and ω_z is the axial frequency. A measure of the trap anisotropy is given by the parameter $\alpha \equiv \omega_z^2/\omega_r^2$; for given N the crystal structure depends only on α. Although the system is now inhomogeneous in z, structures analogous to the 1D chain, the zigzag, and the helix are still observed. In particular, one set of simulations [8] finds that for small α the ions form an inhomogeneous 1D chain along the trap axis, but as α increases, at some point $\alpha_1(N)$ a zigzag structure develops for ions near the trap center, and at a larger value $\alpha_2(N)$ the zigzag twists to form an inhomogeneous finite-length helix. For still larger values of α concentric spheroidal shell structures appear [7,9]. For $\alpha > 1$ the spheroidal structures become oblate and finally at some value $\alpha_3(N)$ they collapse into the x-y plane, forming a distorted 2D hexagonal lattice.

It is important to understand how and when these transitions occur in an inhomogeneous crystal; for example, the performance of an atomic clock based on an inhomogeneous 1D chain depends crucially on trapping many ions and holding them along the axis in the 1D chain configuration [3]. Although empirical scaling laws of the form $\alpha_i(N) \sim N^{p_i}$, p_i a real number, were obtained from the numerical simulations [8], a theory for these power laws was not put forward. In this paper we develop a simple model for the occurrence of these structural transitions which matches the large N simulation results; however, we find that only for α_3 is the above power law form correct. In the process we analytically determine how the length L of an inhomogeneous 1D chain varies with N. We find that a proper explanation of this variation requires a theory which keeps the correlations between the ions, and we employ the local density approximation [10] to take these correlations into account.

Furthermore, in order to explain $\alpha_3(N)$ we also explore the structural transitions of a 2D homogeneous system confined in the x-y plane by a potential $m\omega_z^2 z^2/2$. Although it is well known for sufficiently large ω_z the charges form a single 2D hexagonal lattice plane, the structures which arise as ω_z is lowered have not been previously determined. Here we predict them through both a minimum energy analysis and a stability analysis.

We first consider the zigzag and helical transitions which occur in the inhomogeneous chain confined by the harmonic potential $\phi(r,z)$. When the spacing a between charges is constant, Eq. (1) determines the transition points. Now, however, $a = a(z)$ so we make the simplest possible approximation: In the finite confined system the

0031-9007/93/71(17)/2753(4)$06.00

transitions occur at the point where $a(z)$ decreases below the bounds set by Eq. (1). This predicts that the transitions should occur at the center of the chain where the spacing is smallest, and indeed this is what is observed in the simulations.

In order to find the transition point we need to find the axial spacing $a(z)$, or in particular $a_{\min} = \min[a(z)]$. As the simplest first approximation, we replace the chain of N charges by a charged fluid with total charge Nq. This globule of fluid assumes some equilibrium shape and density in the external potential ϕ and we calculate $a(z)$ as the inverse of the charge per unit length along the z axis of the globule.

Although this is a well-posed problem for a general trap geometry, we are particularly fortunate in that the equilibrium of a charged fluid in a harmonic potential has been previously calculated [11]. The fluid assumes a uniform density n_0 since the harmonic confining potential can be thought of as being produced by a uniform neutralizing background charge of number density $n_0 = \nabla^2\phi/4\pi q^2 = (1+2/\alpha)a_0^{-3}$, where $a_0 \equiv (4\pi q^2/m\omega_z^2)^{1/3}$ is a scale length on order of an ion-ion spacing when $\alpha \gtrsim 1$ (note that ϕ has a nonzero Laplacian as it is not entirely of electrostatic origin [1-4]). In equilibrium the fluid matches its density to n_0. The shape of the fluid globule is a spheroid of length $2L$ and diameter $2R$ where the ratio $\beta \equiv R/L$ is a known function of α [11]:

$$\alpha = A(\beta)/[1 - A(\beta)/2]\,, \tag{2a}$$

where A is a function proportional to the z component of the self-electric-field in the spheroid:

$$A(\beta) = \beta^2\{\ln[(1+k)/(1-k)] - 2k\}/k^3\,, \tag{2b}$$

and where $k \equiv \sqrt{1-\beta^2}$. Equations (2), together with the relation $N = 4\pi R^2 L n_0/3$, determine R and L. In the small α (small β) limit $A(\beta) \to 2\beta^2[\ln(2/\beta) - 1]$ and these equations yield the following result for the length $2L$ of the highly prolate spheroid:

$$L^3 = 3Na_0^3[\ln(32\pi L^3/3N\alpha a_0^3)^{1/2} - 1]/4\pi\,. \tag{3}$$

Now, the number of charges per unit length along the axis of a spheroid is given by

$$1/a(z) = \frac{3}{4}\frac{N}{L}[1 - z^2/L^2]\,, \tag{4}$$

so the minimum value of $a(z)$ occurs at $z=0$ and is equal to $a_{\min} = 4L/3N$. An inhomogeneous zigzag or helical instability will set in when $a_{\min}$ falls below the bounds set by Eq. (1). This implies a limit for L, which when substituted into Eq. (3), yields the following equation for $\alpha_i(N)$:

$$\alpha_i(N) = \left[\frac{8}{3x_iN}\right]^2 [\ln(3Nx_i/2^{3/2}) - 1]\,, \quad i = 1,2\,. \tag{5}$$

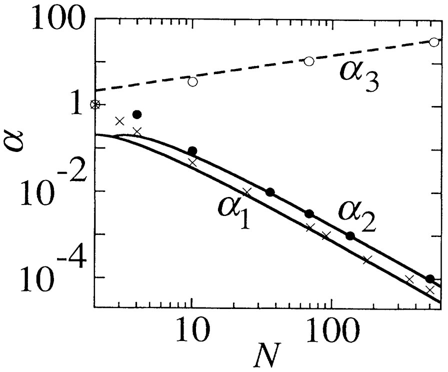

FIG. 1. Locations $\alpha_1(N)$, $\alpha_2(N)$, and $\alpha_3(N)$ of the inhomogeneous zigzag, helical, and planar phase transitions, respectively. Solid lines: Eq. (5) for α_1 and α_2. Equation (10) for α_1 is also plotted, but it cannot be distinguished from Eq. (5). Dashed line: Eq. (7) for α_3. Crosses, solid points, open points: simulation results of Ref. [8] for zigzag, helical, and planar transitions, respectively.

This equation is a good match to the numerical results of Ref. [8] at large N (see Fig. 1). However, the large N logarithmic scaling of Eq. (5) differs from the power law estimates of Ref. [8].

Turning now to the transition from an oblate structure to a 2D system confined in the x-y plane we again employ an approach based on the transitions in an infinite homogeneous lattice, this time a 2D lattice of number density σ per unit area confined by the potential $m\omega_z^2 z^2/2$. The structural transitions of this system have not been previously explored but can be determined by employing known results for the correlation energy E_{corr} of systems of P lattice planes bounded in z by this harmonic potential [12]. The correlation energy is the actual energy minus the energy in the fluid approximation.

In this theory, discussed in detail in Ref. [12], it is shown that E_{corr} is determined solely by the value of P, the 2D lattice type within each plane, and the dimensionless parameter σa_0^2. The main simplifying assumption is that each lattice plane has the same symmetry. The configuration of minimum energy is found by comparing E_{corr} as a function of P and σa_0^2 for several 2D lattice types. By employing the equation for E_{corr} derived in Ref. [12], we have found that the single 2D hexagonal lattice plane is no longer the minimum energy state when σa_0^2 increases beyond $\sigma a_0^2 = w_1$, where $w_1 = 1.11\ldots$ (w_1 is the first 2D transition value, analogous to the 1D transition value x_1). Just beyond this point the minimum energy state consists of three closely spaced 2D hexagonal lattice planes, each with density $\sigma/3$, as shown in the legend of Fig. 2. The z position of the planes as a function of σ is also exhibited in this figure.

This three plane configuration arises from the single plane state through an instability of the 2D lattice. We study the instability by calculating the lattice normal modes. We linearize the equations of motion of the ions about their equilibrium positions $\mathbf{p}$ in a hexagonal lattice, where $\mathbf{p} = [(m+n/2)\hat{\mathbf{x}} + \sqrt{3}n\hat{\mathbf{y}}/2]a_{\text{lat}}$, m and n are integers, and $a_{\text{lat}} = (2/\sqrt{3}\sigma)^{1/2}$ is the lattice constant. By

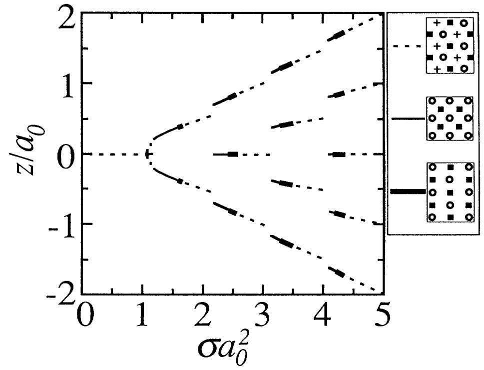

FIG. 2. Minimum energy configurations (lattice type and z position of lattice planes) versus the number of charges per unit area, σ, in a 2D system of ions confined by the potential $m\omega_z^2 z^2/2$. Within each plane one of three lattice types occurs; dashed line: 2D hexagonal; thin solid line: square; thick solid line: bcc 110. Structures are shown in the legend; different symbols refer to ions in different planes.

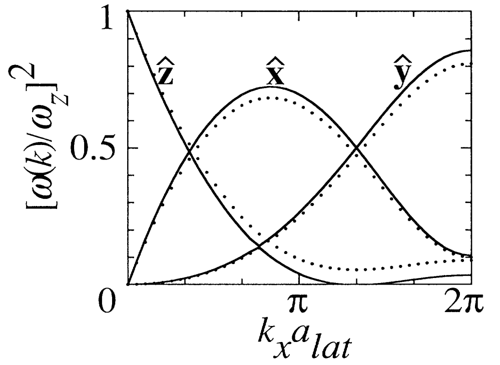

FIG. 3. Frequencies $\omega(\mathbf{k})$ of the three normal modes for a 2D hexagonal lattice, density σ per unit area, confined in the x-y plane by a potential $m\omega_z^2 z^2/2$. Here $k_y=0$ and $k_x a_{\text{lat}}$ runs between 0 and 2π, where the lattice constant $a_{\text{lat}} \equiv (2/\sqrt{3}\sigma)^{1/2}$. Solid lines: $\sigma a_0^2 = 1.11$; dotted lines: $\sigma a_0^2 = 1.07$. Labels $\hat{\mathbf{x}},\hat{\mathbf{y}},\hat{\mathbf{z}}$ refer to mode polarizations.

taking the ion displacements proportional to $\exp(i\mathbf{k}\cdot\mathbf{p})$ where $\mathbf{k}$ is a wave vector in the x-y plane, some algebra then reveals that the square of the normal mode frequency, $\omega^2(\mathbf{k})$, is an eigenvalue of the three-dimensional matrix $\mathbf{A}(\mathbf{k})$ where

$$\mathbf{A}(\mathbf{k}) = q^2/(mN) \sum_{\mathbf{p}}{}' [1-\cos(\mathbf{k}\cdot\mathbf{p})] \times (3\mathbf{pp} - \mathbf{1}p^2)/p^5 + \omega_z^2 \hat{\mathbf{z}}\hat{\mathbf{z}} \,,$$

$\mathbf{1}$ is the 3D unit matrix, and the sum excludes $\mathbf{p}=0$. For any $\mathbf{k}$ there are three polarizations given by the eigenvectors of $\mathbf{A}$. One polarization is always in the z direction; the other two are in the x-y plane. When $k_y=0$, the latter two modes have polarizations in the $\hat{\mathbf{x}}$ and $\hat{\mathbf{y}}$ directions corresponding to compressional and transverse oscillations, respectively. Frequencies of the three modes are shown in Fig. 3 along the $k_y=0$ line for two values of σa_0^2 near instability. At $k_y=0$, $k_x a_{\text{lat}} = 4\pi/3$, the $\hat{\mathbf{z}}$ polarization induces displacements corresponding to the three hexagonal planes shown in Fig. 2; this mode becomes unstable when $\sigma a_0^2 = w_1$.

At still larger values of σa_0^2 the three hexagonal lattice planes are no longer the minimum energy state. At $\sigma a_0^2 = w_2 = 1.15$ they are replaced by two lattice planes with square symmetry (see Fig. 2); no instability develops in this case as the new equilibrium is a separate local minimum in the correlation energy function. At $\sigma a_0^2 = w_3 = 1.57$ the two plane state is replaced by another two plane state, in this case a state in which each plane has the symmetry of bcc (110) lattice planes as shown in Fig. 2. States further along in the sequence are also displayed.

We will use the first 2D transition to describe the structural transition at $\alpha_3(N)$ which is observed in the simulations. We again assume that in the finite system where $\sigma=\sigma(r)$, the inhomogeneous transition occurs when $\sigma(r)a_0^2 = w_1$. Replacing the N charges by a uniform spheroid, in this fluid approximation the number density per unit area varies as

$$\sigma(r) = (3N/2\pi R^2)\sqrt{1-r^2/R^2} \,, \tag{6}$$

where R is found by using Eq. (2) in the oblate ($\alpha,\beta \gg 1$) limit: $R^3 = 3\alpha N a_0^3/16$. When the maximum value of $\sigma(r)$, $3N/2\pi R^2$, is used in the instability criterion we obtain the following scaling law for $\alpha_3(N)$:

$$\alpha_3(N) = (96N/\pi^3 w_1^3)^{1/2} \,. \tag{7}$$

Equation (7) is plotted in Fig. 1 along with the data taken from Fig. 4(b) of Ref. [8] for this transition; the fit is good at large N and the $N^{1/2}$ scaling of the result is very close to the $N^{0.52}$ scaling proposed in Ref. [8].

The phase consisting of a pair of square lattice planes has also been observed in the center ($r/R \lesssim 0.7$) of an oblate crystal at $N=500$ at $\alpha=20$ [8]. These N and α values imply that $\sigma(r=0)a_0^2 = 1.57$. The square phase is stable for $1.15 < \sigma a_0^2 < 1.57$, so Eq. (6) predicts that this phase appears for $r/R < 0.68$, consistent with the simulation.

Finally, we return to an important problem inherent in Eq. (3) which we have not previously mentioned: Equation (3) implies that the length of a 1D Coulomb chain depends on the *radial* confining force, and in particular as $\omega_r \to \infty, L \to \infty$. This problem arises because the fluid approximation does not work for a 1D system: A line charge has infinite fluid energy. In other words, the discreteness of the 1D chain must be taken into account. To see this in another way, note that the total energy of a 1D system scales roughly as q^2N^2/L, whereas the correlation energy is of the same order, scaling as $Nq^2/a \sim Nq^2(N/L)$, so discreteness cannot be neglected. (This is not true in higher-dimensional Coulombic systems of size L since discreteness energy scales as $Nq^2N^{1/D}/L$ for dimension D.)

Correlations can be accounted for by recourse to a 1D version of the local density approximation (LDA) [10]. In this approximation we develop an expression for the correlation energy of the inhomogeneous crystal based on the energy of an infinite 1D chain. For an infinite chain with interparticle spacing a the correlation energy E_{corr} is the difference between the energy of the actual discrete system and the energy of a uniform fluid cylinder of radius R_0 with density per unit length equal to $1/a$. This energy difference can be calculated through the use of Ewald techniques in the spirit of Ref. [13] (note, however, that in Ref. [13] E_{corr} is defined differently); the result is

$$E_{\text{corr}} = \frac{Nq^2}{a}\left[\gamma - \frac{1}{4} + \ln(R_0/2a)\right], \tag{8}$$

where $\gamma = 0.577\ldots$ is Euler's constant.

The correlation energy of the finite system is then calculated in the LDA as a density-weighted average of Eq. (8): $\langle E_{\text{corr}}\rangle = N^{-1}\int dz\, a^{-1}(z) E_{\text{corr}}[a(z)]$, and we now consider Eq. (4) as a trial variational function for $a(z)$ with a single parameter L, equal to half the chain length. This $a(z)$ implies that the uniform fluid cylinder is replaced by a spheroid, so in Eq. (8) R_0 is replaced by $(1 - z^2/L^2)^{1/2}$. The integral can be performed analytically, yielding

$$\langle E_{\text{corr}}\rangle = \frac{3}{5}\frac{q^2}{L}N^2[\gamma - 13/5 + \ln(3NR/L)]\,.$$

This average correlation energy can be used to find the length $2L$ of the chain of charges by minimizing the total energy E of the system with respect to the variational parameter L. The energy is a sum of potential energies due to the harmonic well and the Coulomb self-energy: $E = Nm\omega_z^2\langle z^2\rangle/2 + U_c$, where $U_c = q^2\sum_{i>j}|z_i - z_j|^{-1}$, and $\langle z^2\rangle = L^2/5$ by Eq. (4). We then break U_c up into two pieces: $U_c = U_f + (U_c - U_f)$ where U_f is the fluid self-energy of the spheroid [14]: $U_f = 3q^2N^2\{2 + [\beta^2 - 1] \times A(\beta)\}/10L$. Next, we approximate the correlation energy $U_c - U_f$ by $\langle E_{\text{corr}}\rangle$. Using the $\beta \gg 1$ limit of A and setting $\partial E/\partial L = 0$ yields an expression for L which is independent of R:

$$L^3 = 3Na_0^3[\ln(6N) + \gamma - 13/5]/4\pi\,. \tag{9}$$

This expression solves the problem inherent in Eq. (3): Now the 1D chain length $2L$ is independent of the radial force, as it should be. Equation (3) is not independent of ω_r because there we approximated the line of charges by a fluid of finite radial extent. Thus, Eq. (3) describes the approximate length of the zigzag and helical phases and Eq. (9) describes the 1D chain.

However, when Eq. (9) is used in Eq. (4) to obtain the minimum lattice spacing a_{min}, and when this result is employed in Eq. (1), the result for the zigzag transition is almost identical to the simple fluid model:

$$\alpha_1(N) = \left(\frac{8}{3x_1N}\right)^2[\ln(6N) + \gamma - 13/5]\,. \tag{10}$$

It is heartening that Eqs. (5) and (10) provide nearly identical results for $\alpha_1(N)$. This is not a coincidence: At the zigzag transition the lengths of the zigzag phase [Eq. (3)] and the 1D chain [Eq. (9)] *should* be equal, so Eqs. (5) and (10) should also give equal values for α_1. Both equations are approximate: Equation (5) neglects correlations whereas Eq. (10) keeps correlations in the LDA with a single parameter trial variational function. A more accurate version of the LDA involves a numerical solution of the variation problem $\delta E/\delta a(z) = 0$. Results of this analysis will be presented elsewhere.

We have derived economical expressions for the zigzag, helical, and planar transitions of an inhomogeneous Coulomb crystal. Our expressions match the large N results of recent computer simulations [8], but our scaling laws for the zigzag and helical transitions [Eqs. (5) and (10)] differ from the power law forms put forward in Ref. [8]. We have also employed the local density approximation to determine the length $2L$ of the inhomogeneous 1D Coulomb chain. Our results for $L(N)$ and $\alpha_1(N)$, Eqs. (9) and (10), can be used to find the trap fields required to hold a 1D chain of given number and length. Finally, we have predicted the planar structures which should be observed in a highly oblate crystal. They consist of stacked hexagonal, square, or bcc 110 lattice planes, depending sensitively on the values of α and N. Only two of these planar structures—the single plane hexagonal lattice and the two plane square lattice—have yet been observed in simulations or experiments.

This work was supported by National Science Foundation Grant No. PHY91-20240 and ONR Grant No. N00014-89-J-1714.

[1] S. L. Gilbert, J. J. Bollinger, and D. J. Wineland, Phys. Rev. Lett. **60**, 2022 (1988).

[2] F. Diedrich *et al.*, Phys. Rev. Lett. **59**, 2931 (1987); D. J. Wineland *et al.*, Phys. Rev. Lett. **59**, 2935 (1987).

[3] M. G. Raizen *et al.*, Phys. Rev. A **45**, 6493 (1992).

[4] G. Birkl, S. Kassner, and H. Walther, Nature (London) **357**, 310 (1992).

[5] H. Totsuji and J.-L. Barrat, Phys. Rev. Lett. **60**, 2484 (1988).

[6] R. W. Hasse and J. P. Schiffer, Ann. Phys. (N.Y.) **203**, 419 (1990).

[7] A. Rahman and J. Schiffer, Phys. Rev. Lett. **57**, 1133 (1986).

[8] J. P. Schiffer, Phys. Rev. Lett. **70**, 818 (1993).

[9] D. H. E. Dubin and T. M. O'Neil, Phys. Rev. Lett. **60**, 511 (1988); R. Rafac *et al.*, Proc. Natl. Acad. Sci. **88**, 483 (1991); R. Hasse and Ul. Avilov, Phys. Rev. A **44**, 4506 (1991).

[10] P. Hohenberg and W. Kohn, Phys. Rev. **136**, B864 (1964).

[11] L. Turner, Phys. Fluids **30**, 3196 (1987).

[12] D. H. E. Dubin, Phys. Rev. A **40**, 1140 (1989).

[13] H. Totsuji, Phys. Rev. A **38**, 5444 (1988).

[14] D. H. E. Dubin, Phys. Fluids B **5**, 295 (1993).